[11]H. Unoki and T. Sakudo, J. Phys. Soc. Japan 23, 546 (1967).
[12]J. C. Slonczewski and H. Thomas, Phys. Rev. B 1, 3599 (1970).
[13]K. A. Müller and W. Berlinger, Phys. Rev. Letters 26, 13 (1971).
[14]K. A. Müller, W. Berlinger, and J. C. Slonczewski, Phys. Rev. Letters 25, 734 (1970).
[15]K. A. Müller, Helv. Phys. Acta 31, 173 (1958).
[16]K. A. Müller, W. Berlinger, M. Capizzi, and H. Gränicher, Solid State Commun. 8, 549 (1970).
[17]B. Alefeld, Z. Physik 222, 155 (1969).
[18]D. A. Jones, J. M. Baker, and D. F. D. Pope, Proc. Phys. Soc. (London) 74, 249 (1959).
[19]B. Henderson, J. E. Wertz, T. P. P. Hall, and R. D. Dowsing, J. Phys. C 4, 107 (1971).
[20]See, for instance, E. U. Condon and G. H. Shortley, *The Theory of Atomic Spectra* (Cambridge U. P., Cambridge, 1957), p. 34.
[21]K. A. Müller, in *Structural Phase Transitions and Soft Modes*, edited by E. J. Samuelsen, E. Andersen, and J. Feder (Universitetsforlaget, Oslo, Norway, 1971), p. 85.
[22]F. Schwabl, Phys. Rev. Letters 28, 500 (1972).
[23]Th. von Waldkirch, K. A. Müller, W. Berlinger, and H. Thomas, Phys. Rev. Letters 28, 503 (1972).

PHYSICAL REVIEW B VOLUME 5, NUMBER 11 1 JUNE 1972

Determination of the Sternheimer Antishielding Factor of Li^7 in Lithium Fluoride by Acoustic Nuclear Magnetic Resonance*

J. R. Anderson† and J. S. Karra
Department of Physics, Temple University, Philadelphia, Pennsylvania 19122
(Received 2 August 1971)

An experimental determination of the magnitude of the Sternheimer antishielding factor $1-\gamma_\infty$ for the Li^+ ion by means of acoustic nuclear magnetic resonance (acoustic NMR) of Li^7 in single-crystal LiF is presented. It was found that $|1-\gamma_\infty| = 3.4 \pm 13\%$, corresponding to an antishielding effect. This may be compared with theoretical calculations by other investigators which give $1-\gamma_\infty = 0.75$, a small shielding effect. The shape of the acoustic NMR line for H parallel to the [001] direction was found to be approximately Gaussian with a second moment $\Delta H^2 = (5.1 \pm 0.8)^2\ G^2$. A theoretical calculation of that second moment was carried out, assuming only magnetic dipole-dipole interactions between nuclei, and yielding $\Delta H^2 = 5.9\ G^2$ in good agreement with this experiment. Experimentally, the LiF crystal was cooled in liquid helium to 4.2°K and placed in a steady magnetic field H. Acoustic waves at twice the Li^7 Lamor frequency were introduced into the crystal by means of a piezoelectric transducer. The resulting periodic distortions of the crystal modulated the interaction $\overleftrightarrow{Q}:\nabla\vec{E}$ between the nuclear electric quadrupole moment $\overleftrightarrow{Q}$ and the electric-field gradient $\nabla\vec{E}$ generated transitions among the Zeeman energy levels. These transition rates were measured by observing the rate of change of the amplitude of an ordinary (nonacoustic) NMR signal. The transition rate expected for a point-charge model of the crystal was calculated to be proportional to $(\overleftrightarrow{Q}:\nabla\vec{E})^2$, and, using the known value $Q = 0.043$ barn, was smaller than the experimental transition rate by a factor of 11.8. Additional calculations were made which showed that covalency and overlap should have a negligible effect on ∇E, making it possible to ascribe this factor of 11.8 solely to antishielding. The ratio of the actual transition rate to that calculated is equal to the square of the antishielding factor: $(1-\gamma_\infty)^2 = 11.8$ so that $|1-\gamma_\infty| = 3.4$, with an estimated probable error of 13%.

I. INTRODUCTION

In this paper we report an experimental determination of the Sternheimer antishielding factor for the Li^7 ion in lithium fluoride. The experiment makes use of the method of ultrasonic saturation of the lithium NMR line.

This method was first conceived by Kastler[1] and entails the modulation of the quadrupole coupling energy by means of acoustic waves at the proper frequency to generate transitions among the nuclear Zeeman states. This effect, first demonstrated by Proctor and Tantilla[2] and later by other investigators[3–12] is observed in two different experimental forms. One, the dissipation method, which was developed by Bolef and Menes,[7,8] makes use of the marginal oscillator as in ordinary NMR. The other is the saturation method, used in this present experiment, which depends on the saturation of NMR lines as a consequence of the transitions induced by the acoustic effect.

In the saturation method, one observes the time rate of decrease dS/dt of the NMR signal S. Then if M is the magnetization of the sample,

$$\frac{1}{S}\frac{dS}{dt} = \frac{1}{M}\frac{dM}{dt} = KP\ , \tag{1}$$

where the latter equality depends on the existence

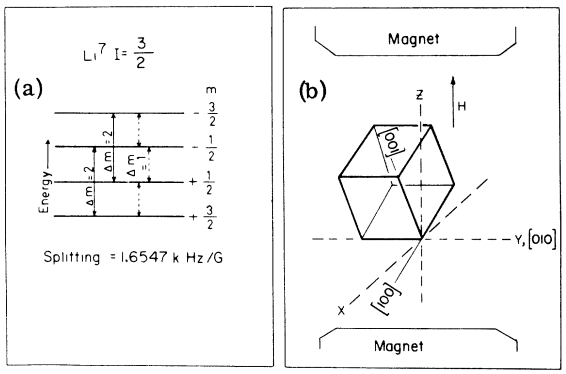

FIG. 1. Cubic crystal of LiF in a steady magnetic field H. (a) Zeeman energy levels of the Li^7 nucleus. The $\Delta m = \pm 1$ and $\Delta m = \pm 2$ transitions are indicated by the dashed and solid lines, respectively. (b) Coordinate system and orientation of the crystal in the magnetic field. The X, Y, and Z axes are fixed in space with H along Z. The crystal [010] axis coincides with Y and the crystal may rotate about it through the angle θ. At $\theta = 0$ the crystal [100] and [001] axes coincide with X and Z, respectively. The transducer is cemented on the (100) face.

of a spin temperature, P is the transition rate between two nuclear Zeeman levels involved in the process, and K is a small number depending only on the nuclear spin I and the two particular energy levels selected. It is possible to calculate P directly, given knowledge of the dynamic quadrupole coupling energy $\overleftrightarrow{Q}$: $\nabla\vec{E}(t)$, where $\overleftrightarrow{Q}$ is the nuclear electric quadrupole tensor and $\nabla\vec{E}$ is the electric-field gradient at the nucleus. Knowledge of $\overleftrightarrow{Q}$ fixes the value of the component of ∇E appropriate to the particular transition [$\Delta m = \pm 1$ or $\Delta m = \pm 2$, Fig. 1(a)] being induced, but since one knows only (at best) the amplitude, polarization, and direction of the acoustic wave, it is necessary to determine the relation between those latter factors and $\nabla\vec{E}$.

Calculations of $\vec{E}(t)$ on the point-charge model of the lattice have been shown to be inadequate because of the effects of covalency,[13] overlap,[14] and antishielding.[15] Since the experiments do not afford a separation of these effects it has been necessary to calculate their magnitudes, and the accuracy of the results depends on the details of the calculations and the wave functions employed.

In the case of the Li^7 ion in LiF it might be expected that, because of the small structure of the ion and the high ionicity[16] of the bond, covalency and overlap should have a minimal effect. Using the theories of Yosida and Moriya[13] to assess the covalency effect and of Kondo and Yamashita[14] for overlap, we find that both are negligible compared to our experimentally observed deviation in $\nabla\vec{E}$ from that of the point-charge model. Because they are negligible, the absolute accuracy of their calculation is not critical and it is possible to ascribe the deviation in $\nabla\vec{E}$ solely to Sternheimer antishielding.

Since the transition probability goes as $(\nabla\vec{E})^2$ and $\nabla\vec{E} = (1-\gamma_\infty)\nabla\vec{E}_{PC}$, where $\nabla\vec{E}_{PC}$ is the electric-field gradient on the point-charge model, it is possible to determine only the magnitude $|1-\gamma_\infty|$ of the antishielding factor, for which we get a value $|1-\gamma_\infty| = 3.4 \pm 0.4$.

II. THEORY

In this section we calculate the transition rate among the Li^7 nuclei Zeeman states [Fig. 1(a)] as induced by the time-dependent field gradient $\nabla\vec{E}(t)$ created by longitudinal waves in the LiF crystal. We consider only $\Delta m = 2$ transitions and take the point-charge model, augmented by the Sternheimer antishielding factor $(1-\gamma_\infty)$, for $\nabla\vec{E}$. We use the theories of Yosida and Moriya and of Kondo and Yamashita to estimate the effects of covalency and overlap and find that they are negligible. In addition, the second moment of the acoustically observed line shape is calculated for comparison with the experimental results.

A. Transition Rates

The quadrupolar-perturbed Hamiltonian can be written[17]

$$\mathcal{H}_Q = \sum_{\mu=-2}^{+2} Q_\mu W_{-\mu} , \tag{2}$$

where Q and W are the spherical components of the electric quadrupole moment and electric-field-gradient tensors, respectively. For $\Delta m = 2$ transitions we need consider only the $\mu = +2$ term[17]:

$$Q_{+2} = \frac{eQ}{I(2I-1)} \frac{\sqrt{6}}{4} I_+^2 , \tag{3}$$

$$W_{-2} = \frac{1}{2\sqrt{6}} (V_{xx} - V_{yy} - 2iV_{xy}) . \tag{4}$$

The transition rate is given by

$$P_2 = \frac{1}{4\hbar^2} |\langle f|Q_{+2}W_{-2}|i\rangle|^2 g(\nu) , \tag{5}$$

where $g(\nu)$ is the normalized line-shape function and $|i\rangle$ and $|f\rangle$ are the initial and final states of the system. We now follow the theory and notation of Van Kranendonk[18] and arrive at the following expression for the $\Delta m = 2$ transition rate

$$P_2 = \frac{1}{4\hbar^2} \langle Q^2\rangle \sum_{\vec{k}} \langle q_{\vec{k}}^2\rangle k^2 |\sum_i (A_i \cdot \hat{\vec{k}})(\vec{a}_i \cdot \hat{\vec{k}})|^2 g(\nu) , \tag{6}$$

where

$$\langle Q^2\rangle = \left(\frac{eQ}{I(2I-1)} \frac{\sqrt{6}}{4}\right)^2 |\langle m+2|I_+^2|m\rangle|^2 = \tfrac{1}{2}e^2Q^2 \tag{7}$$

for the lithium nucleus, $I = \frac{3}{2}$, and Q is its quadru-

pole moment. We define

$$\langle q_{\vec{k}}^2 \rangle \equiv | \langle n_{\vec{k}} - 1 | q_{\vec{k}} | n_{\vec{k}} \rangle |^2 = \hbar n_{\vec{k}} / M\omega \ , \tag{8}$$

where $n_{\vec{k}}$ is the number of phonons of wave number $\vec{k}$ and angular frequency ω, $q_{\vec{k}}^{\dagger}$ is the annihilation operator, and M is the mass of the crystal. It follows then, that for a cubic crystal, V is the velocity of sound being independent of $\vec{k}$ and direction

$$\sum_{\vec{k}} \langle q_{\vec{k}}^2 \rangle k^2 = E/2MV^2 \ , \tag{9}$$

where E is the acoustic energy in the crystal. A_i is defined by the expansion of W_{-2} in powers of $\vec{r}_i$, the relative vector displacement from equilibrium of the ith ion from that of central Li nucleus:

$$W_{-2} = A_0 + \sum_i \nabla_i W_{-2} \cdot \vec{r}_i \ , \tag{10}$$

and, finally, $\vec{a}_i$ is the vector between the equilibrium positions of the central nucleus and the ith ion.

The above treatment follows Van Kranendonk's formalism using his notation, but in deriving Eq. (6) we have made adaptations to the conditions of the present experiment: Only longitudinal waves with $\vec{k} \cdot \vec{a} \ll 1$ are considered. This procedure dispenses with the cosine-type waves of Ref. (18) and hence we obtain a 2 in the denominator of Eq. (9): The cosine waves have half the energy but are not effective in inducing transitions.

The electric-field gradient resides in the A_i and we find, after successive differentiation of the potential due to the six nearest neighbors[18a] and including the antishielding factor,

$$A_{ix} = \beta_i' \left(-15 X_i \frac{(X_i - iY_i)^2}{a_i^2} + 6(X_i - iY_i) \right) ,$$

$$A_{iy} = \beta_i' \left(-15 Y_i \frac{(X_i - iY_i)^2}{a_i^2} - 6i(X_i - iY_i) \right) , \tag{11}$$

$$A_{iz} = \beta_i' \left(-15 Z_i \frac{(X_i - iY_i)^2}{a_i^2} \right) ,$$

and

$$\beta_i' = \frac{1}{2\sqrt{6}} \frac{e_i}{a_i^5} (1 - \gamma_\infty) .$$

e_i is the charge on the ith ion and X_i, Y_i, Z_i are the coordinates of the ith ion in the Cartesian frame fixed in space with the z axis along the magnetic field $\vec{H}$ [Fig. 1(b)]. The crystal was oriented with a [010] axis along the fixed y axis and was rotatable about this common direction through the angle θ such that at $\theta = 0$ the [100] and [001] axes coincide with their counterparts in the fixed system. Because P_2 varies as $\sim a_i^2 A_i^2 \propto a_i^{-6}$, we consider only the six-nearest-fluorine neighbors[18a] with internuclear distance $a_0 = 2.01$ Å. We calculate the following quantity:

$$G(\theta) = \sum_i (A_i \cdot \hat{\vec{k}})(\vec{a}_i \cdot \hat{\vec{k}})$$

$$= 2\beta [(-9 + 30 \sin^2\theta \cos^2\theta) \hat{k}_x \hat{k}_y + 9 \hat{k}_y \hat{k}_y$$
$$- 30 \sin^2\theta \cos^2\theta \hat{k}_z \hat{k}_z + 30 \sin\theta \cos\theta$$
$$\times (\cos^2\theta - \sin^2\theta) \hat{k}_x \hat{k}_z - 12 i \hat{k}_x \hat{k}_y] ,$$
$$\beta = \frac{1}{2\sqrt{6}} \frac{e}{a_0^3} (1 - \gamma_\infty) . \tag{12}$$

We now consider two cases. Case I represents longitudinal waves along the crystal (rotating) [100] axis. For this case, we have

$$|G(\theta)|^2 \equiv |G_x(\theta)|^2 = 4\beta^2 (81 \cos^4\theta) , \tag{13}$$

$$P_2 = P_{2x} = \frac{27}{16} \frac{e^4 Q^2}{\hbar^2} \frac{E}{2MV^2 a_0^6} \cos^4\theta g(\nu) (1 - \gamma_\infty)^2 . \tag{14}$$

Case II shows longitudinal waves with isotropic distribution of k vectors:

$$|G(\theta)|^2 = |G_{\rm ISO}(\theta)|^2 = 4\beta^2 \ 12(\tfrac{13}{5} - \sin^2\theta \cos^2\theta) , \tag{15}$$

where it is necessary to calculate $|G_{\rm ISO}(\theta)|^2$ in terms of the components of $\vec{k}$ and use the following averages:

$$\langle k_x^4 \rangle = \langle k_y^4 \rangle = \langle k_z^4 \rangle = \tfrac{1}{5} ,$$
$$\langle k_x^2 k_y^2 \rangle = \tfrac{1}{15} . \tag{16}$$

This yields

$$P_2 = P_{2\,\rm ISO} = \frac{13}{20} \frac{e^4 Q^2}{\hbar^2} \frac{Eg(\nu)}{2MV^2 a_0^6} (1 - \gamma_\infty)^2 , \tag{17}$$

where we ignore the small dependence on θ.

B. Covalency

The Li-F bond is not purely ionic so there is an admixture of covalent orbital around the Li nucleus whose amount depends on the internuclear distance. If this is a p-type electron, it will set up a significant electron-field gradient which then will be modulated by the lattice vibrations. Yosida and Moriya have treated this effect generally and their formalism is quite similar to Van Kranendonk's. The calculations are straightforward and we get, for the transition rate due to this effect,

$$P_{\rm cov} = \frac{1}{4\hbar^2} \langle Q^2 \rangle \sum_{\vec{k}} \langle q_{\vec{k}}^2 \rangle k^2 B^2 (4 a_0 \lambda'^2) \cos^4\theta g(\nu) , \tag{18}$$

where the new quantities to be defined are

$$B \equiv \frac{3e}{5\sqrt{6}} \left\langle \frac{1}{r^3} \right\rangle , \quad \lambda' = \frac{\partial \lambda(R)}{\partial R} ,$$

$\langle 1/r^3 \rangle$ is the expectation value over the covalent orbital and R is the interionic distance in Å. λ is the degree of covalency between the central Li ion and the nearest-neighbor F ion: It is essentially the square of the coefficient of the covalent orbital in the total wave function. Yosida and Moriya take $\lambda(R) = \lambda_0 \exp(-R/0.345)$. For the pres-

ent case we take $\lambda(a_0) = 0.014$, the total covalency given by Phillips[16] divided by the coordination number. Considering the extreme case where the covalent orbital is wholly $2p$, we have from Barnes and Smith[19] $\langle 1/r^3 \rangle = 0.38$ Å^{-3}. Numerically we find $P_{COV} \approx 10^{-4} P$ (point charge) and so the covalent contribution is completely negligible. Even a covalency several times larger would not change the qualitative result, which is due primarily to the small value of $\langle 1/r^3 \rangle$. In contrast, the same calculation for I^{127} in KI gives

$$\langle 1/r^3 \rangle = 122 \text{ Å}^{-3}, \quad P_{COV} = 6 \times 10^3 P \text{ (point charge)}.$$

C. Overlap

The formal theory of the overlap contribution to the transition rate is, as Kondo and Yamashita note, identical to that for the covalent effect even as far as the numerical coefficients. The only difference comes in the identification of λ with the square of the overlap integral $|S_{\mu\nu}|^2$, where

$$S_{\mu\nu} = \int \phi_\mu^* \phi_\nu d\tau$$

and ϕ_μ and ϕ_ν are the relevant wave functions of the two ions. Those authors use the ground-state free-ion wave functions, but for lithium this is a $1S$ wave function for which the expectation value of the field gradient vanishes. This implies that, within their approximation, the overlap effect vanishes as well.

D. Second Moment

We calculate the second moment of the resonance line by the method of Van Vleck. We consider as perturbations on the Zeeman energies, the Li-Li and Li-F dipole-dipole interactions. This is a special case of the more general moment calculations of Loudon[20] and Sundfors.[21] We have

$$\langle \Delta E^2 \rangle = \mathrm{Tr} \frac{[(\mathcal{H}_{DIP}, I_+^2)^2]}{\mathrm{Tr}[(I_+^2)^2]}$$

$$= \frac{45}{8} \frac{\gamma_{Li}^4 \hbar^4}{a_0^6} \sum_p \left(\frac{1}{R_p^3} (1 - 3\cos^2\theta_p) \right)^2 + \frac{\gamma_{Li}^2 \gamma_F^2}{a_0^6} \sum_l \left(\frac{1}{R_l^3} (1 - 3\cos^2\theta_l) \right)^2, \quad (19)$$

where γ_{Li}, γ_F are the Li, F gyromagnetic ratios and R_p, θ_p; R_l, θ_l are the distances and polar angles between the central nucleus and the pth Li nucleus; lth F nucleus, respectively, and H is along the [001] axis. Summing over nuclei out to a distance $8a_0$ gives

$$\langle \Delta H^2 \rangle = \frac{1 \langle \Delta E^2 \rangle}{4 \gamma_{Li}^2 \hbar^2} = 5.9 \text{ G}^2.$$

This is to be compared with the experimental value of $\Delta H^2 = 5.1$ G^2 discussed later.

III. EXPERIMENTAL

The experimental procedure consisted of measuring the relative magnitude of the Li^7 NMR signal from single-crystal LiF before and after introducing the acoustic waves. The two crystals studied were obtained from semielements and Harshaw and were cylindrical, 0.64 cm in diameter and 1.27 (sample I) and 2.75 (sample II) cm in length with (100) end faces and the cylinder axes in the [100] direction. The Li^7 relaxation time T_1 was adjusted to a convenient value of a few min at 4.2 °K by producing paramagnetic F centers in the crystals with x irradiation.

The piezoelectric transducers were of Clevite PZT-5, 0.64 cm in diameter with an active area 0.45 cm in diameter, and were poled so as to produce compression waves at a fundamental frequency of 10 MHz. The transducers were affixed to the crystals with "Non-Aq" stopcock grease and inserted into a holder, around which the NMR coils were wrapped. They were driven at the fundamental and third harmonic and the exact frequencies were chosen to coincide with a mechanical resonance of the sample so as to provide the most efficient coupling of energy into the sample. These frequencies were determined by placing the transducer sample system in parallel with an LC tank circuit, sweeping the frequency across resonance and noting at what frequencies increased dissipation reduced the Q of the circuit. Figure 2 shows such a resonance curve for sample I around 30 MHz. The dips are spaced 257 kHz apart, in agreement with the spacing calculated from the sound velocity. From the large reduction in the electrical Q accompanying mechanical resonance of the sample, we conclude that the energy finally dissipated as heat originally entered the crystal as acoustic waves.

The magnetic field $\vec{H}$, parallel to the crystal [100] axis ($\theta = 0°$) was adjusted so that the frequency of a mechanical resonance was twice the Larmor

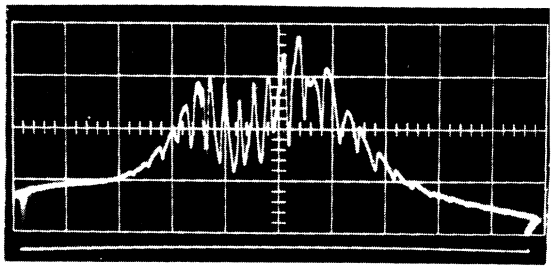

FIG. 2. Oscilloscope trace of the voltage developed across the LC tank circuit formed in part by the transducer sample assembly as the frequency sweeps from left to right across resonance. The deep dips correspond to mechanical resonance of the sample.

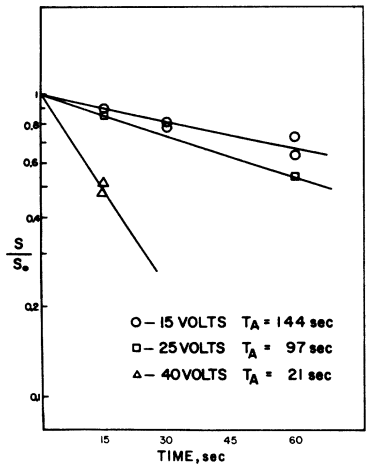

FIG. 3. Decay of signal height in sample II due to acoustic irradiation.

frequency of Li^7. The marginal oscillator, built from the design of Robinson,[22] was run at a very low level of rf field (~ 0.3 mG) to avoid saturation. At time $t=0$ the NMR signal height $S(0)$ was measured, the marginal oscillator was shifted off resonance and the acoustic power was applied for time t_0. Then $S(t_0)$ was immediately measured, T_1 being long enough to permit this to be done accurately. The rate of change of the magnetization can be written

$$\dot{M} = -\tfrac{3}{2}\dot{n}(\tfrac{3}{2}) - \tfrac{1}{2}\dot{n}(\tfrac{1}{2}) + \tfrac{1}{2}\dot{n}(-\tfrac{1}{2}) + \tfrac{3}{2}\dot{n}(-\tfrac{3}{2}) , \quad (20)$$

where $n(\frac{3}{2})$ is the population of the $m=\frac{3}{2}$ level, etc. With spin-spin interactions maintaining a spin temperature (Ref. 17, p. 140) it is easy to show that under the acoustically driven $\Delta m = 2$ transitions M will decay exponentially with a time constant T_A given by

$$1/T_A = \tfrac{8}{5}P , \quad (21)$$

where P is the $\Delta m = 2$ transition rate. With S proportional to M we then have

$$\frac{dS(t)}{dt} = -\frac{1}{T_A}S(t) + \frac{1}{T_1}[S_0 - S(t)] , \quad (22)$$

where the second term on the right-hand side accounts for relaxation back to the equilibrium signal height S_0. For sample II that the second term was always much smaller than the first, and T_A could be determined from a plot of $\ln(S/S_0)$ vs t (Fig. 3). For sample I (Fig. 4) $T_A \simeq T_1$ and Eq. (22) must be integrated, yielding an implicit equation for T_A:

$$\frac{S_0 - T_1(1/T_1 + 1/T_A)S(t_0)}{S_0 - T_1(1/T_1 + 1/T_A)S(0)} = \exp\left[-\left(\frac{1}{T_1} + \frac{1}{T_A}\right)t_0\right] , \quad (23)$$

which was solved graphically for T_A.

Although driving the transducer at twice the Larmor frequency should prohibit any magnetic dipole transitions, a check was made during each run by performing an identical experiment on the F^{19} nuclei, which have no quadrupole moment. Only H was changed to conform to γ_F, and in each case there was no effect on the F^{19} signal due to the acoustic waves.

Further necessary data are the energy content E and the sound velocity V. A short pulse of sound was injected into the sample and its attenuation on successive reflections gave the phonon lifetime while V could be inferred from the time between successive reflections. We found $V = 6.4 \times 10^5$ cm/sec, within 2% of that calculated from the compressibility and for sample I, $\tau = 5.5$ μsec, sample II $\tau = 35$ μsec. The total acoustic power delivered to the crystal was determined by measuring the excess rate of helium boiloff during acoustic irradiation. The energy content was just the product of power and phonon lifetime. The experimental errors associated with the measurements were estimated to be ~ 2% for V, ~ 10% for T_A, and ~ 20% for the power. The latter error stemmed from the cooling of the upper part of the dewar during the period of excess flow when the power was on. As a result the excess helium was not completely expanded to room temperature and continued to evolve for a short time after the power was cut off.

The line-shape function $g(\nu)$ was determined by measuring T_A for various values of H about H_0, the magnetic field corresponding to the double Larmor frequency, and with $\vec{H}$ parallel to the

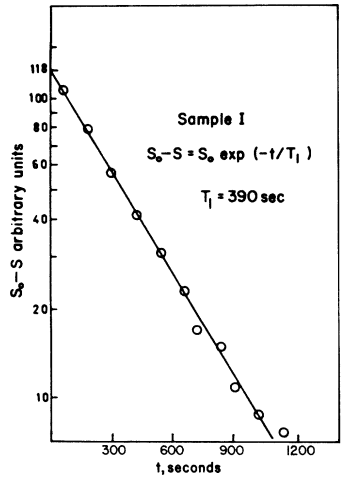

FIG. 4. Polarization curve for sample I. The magnetic field is turned on at time $t=0$ and the NMR signal height subsequently goes as $S = S_0(1 - e^{-t/T_1})$, from which we obtain S_0 and T_1.

TABLE I. Acoustic transition rates of LiF vs acoustic power.

Sample I

$\tau = 5.5$ μsec, $T_1 = 390$ sec,
acoustic frequency ≈ 30 MHz, mass = 0.96 g.

Run	Transducer V, p-p	T_A sec	Power erg/sec	E erg	E/M erg/g
1	18	337	8.5×10^5	4.7	4.9
2	18	350	8.5×10^5	4.7	4.9
3	21	322	1.1×10^6	6.1	6.4
4	24	229	1.4×10^6	7.2	7.5
5	24	240	1.4×10^6	7.2	7.5
6	26	227	1.6×10^6	9.1	9.5

Sample II

$\tau = 35$ μsec, $T_1 = 840$ sec,
acoustic frequency = 10 MHz, mass = 2.28 g.

Run	Transducer V, p-p	T_A sec	Power erg/sec	E erg	E/M erg/g
1	15	144	1.1×10^6	38.4	16.9
2	25	97	2.3×10^6	80	35
3	40	21	8.7×10^6	305	134

[100] axis ($\theta = 0°$). The resulting curve of relative transition rate (Fig. 5) is well approximated by a Gaussian, giving a second moment of $\Delta H^2 = 5.1 \pm 0.8$ G^2 which is in good agreement with the value $\Delta H^2 = 5.9$ G^2 calculated in Sec. IID. From the curve we also obtain $g(\nu)_{H=H_0} = (2.38 \pm 0.38)\times10^{-5}\ H_g^{-1}$, where the errors in the latter determinations were estimated by considering the range of Gaussians that could reasonably be drawn through the points in Fig. 5.

IV. RESULTS

Table I gives the various experimental parameters for the several runs on the two crystals, and from Eq. (21) we obtain, for the experimentally determined transition rate,

$$P_E = 5/8T_A \tag{24}$$

given in Table II.

Now, Eq. (14) predicts a strong dependence on the angle $\theta = 0°$ and $\theta = 90°$ were identical. Serious deviations from the $\cos^4\theta$ dependence have been observed by various investigators, but only Taylor and Bloembergen[5] in NaCl and Gregory and Bommel[9,10] in metallic Ta seem to have encountered an almost total lack of dependence on θ. The former authors used this observed isotropy to determine the form of the S tensor relating the strain and field-gradient tensors and attribute it to departures from pure ionicity in the crystal. However, they do not explain how such covalency or overlap might bring about the isotropy. The latter authors attributed the lack of angular dependence on the generation of unwanted modes of vibration due to the small ratio of sample dimension to sound wavelength. They support this conclusion with the observation that, after carefully polishing the transducer electrode flat, some angular dependence was indeed observed. There could be no question of interfering magnetic dipole transitions since the $\Delta m = 2$ transition was similarly affected. No other reason presents itself to us and we assume that spurious modes were responsible in the present case. This was the motivation for the calculation of P for the isotropic distribution of k vectors —Eq. (17).

Using Eq. (17) and the known quadrupole moment of Li^7, $Q = 0.043$ b,[23-26] we write

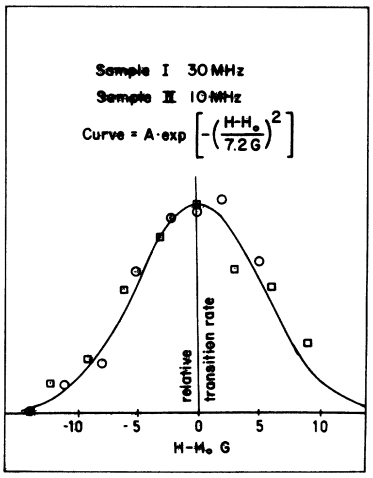

FIG. 5. Acoustic NMR line $\Delta m = 2$ for the two samples. The solid line drawn is a Gaussian curve. The magnetic field is parallel to the [001] axis.

TABLE II. Experimental and theoretical transition rates of LiF. Values of P_E, P_T, P_E/P_T, and $|1-\gamma_\infty|$ for the several runs on the two crystals.

Sample I

Run	$10^3 P_E$[a]	$10^3 P_T$[b]	P_E/P_T	$\lvert1-\gamma_\infty\rvert$
1	1.9	0.128	14.8	3.84
2	1.8	0.128	14.1	3.75
3	1.9	0.168	11.3	3.36
4	2.7	0.196	13.8	3.71
5	2.6	0.196	13.2	3.62
6	2.8	0.248	11.3	3.36

Sample II

1	4.4	0.441	10.0	3.16
2	6.4	0.91	7.0	2.64
3	30	3.52	8.5	2.91

Average value of $|1-\gamma_\infty|$: $|1-\gamma_\infty|_{av} = 3.4$
rms deviation = 0.4

[a] P_E = experimental transition rate from Eq. (24).
[b] P_T = theoretical transition rate from Eq. (14).

$$P_E = P_T(1-\gamma_\infty)^2 \ ,$$

where numerically $P_T = 2.61\times10^5\, E/M$, P_T being the calculated transition rate in the absence of antishielding.

Table II shows the results for the several runs, the last column being the magnitude $|1-\gamma_\infty|$. The average is $|1-\gamma_\infty| = 3.4\pm0.4$, the rms deviation being close to the estimated experimental error ±0.6 for a single run.

The values determined for sample II are found to be somewhat lower than those for sample I, but in view of the rather different experimental parameters in the two cases, crystal mass, phonon lifetime, frequency, etc., the general agreement in results supports the correctness of the value determined for $|1-\gamma_\infty|$.

V. DISCUSSION AND CONCLUSIONS

It was found that the acoustically induced transition rate was some 11 times faster than that predicted theoretically on the point-charge model of the dynamic field gradient. Since calculations based on existing theories show that covalency and overlap have a negligible effect, it is concluded that this augmentation of the field gradient is due to antishielding. Insofar as the state of the two core electrons is not much affected by its chemical environment, this antishielding parameter should be an intrinsic property of the ion and unaffected by its state of chemical combination. The present results are at variance with theoretical calculations of Sternheimer[15] and of Das and Behrsohn,[27] who separately find $1-\gamma_\infty = 0.75$—a small shielding effect. However, it has been pointed out[28,29] that their calculations, although different in approach are equivalent in principle if carried out rigorously, and do not constitute independent determinations.

Calculations by Lahiri and Mukherji[30] and by Langhoff and Hurst[31] give the same results. Although the exact calculated values of the shielding parameter for large ions depend on the form of the wave functions used and on the details of the calculations, there are fairly general reasons for anticipating that for ion cores containing only s electrons there should be a shielding rather than an antishielding effect. This is because in this case, only "angular" excitations are effective in modifying the field gradient. If we accept this principle, then we take the shielding parameter to be negative: $1-\gamma_\infty = -3.4$. Shielding of sufficient magnitude to reverse the sign of the field gradient is theoretically possible, for instance Langhoff and Hurst[31] obtain for Li^- $(1s^2 2s^2)$ $1-\gamma_\infty = -1.64$.

Calculations quoted above are based on free-ion wave functions, but Lahiri and Mukherji[32] point out that in a crystal the electron distribution of the core can be somewhat modified. They cite the case of Li^+ in LiF where such a distortion has been found to exist and from an empirical rule predict a somewhat larger amount of shielding.

We can not here resolve the discrepancy between experiment and theory, but it might reside in the distortion mentioned above. In that case, the antishielding parameter would not be an intrinsic property of the ion, but would depend upon its chemical environment, and it would require accurate wave functions for the crystalline electrons to settle the matter.

ACKNOWLEDGMENT

We acknowledge our gratitude to G. E. Kemmerer for his very willing technical help throughout our experimental work.

---

*Part of this work was submitted in the doctoral thesis to Temple University by J. R. Anderson.

†NASA trainee 1968–70. Present address: Dept. of Physics, Brown University, Providence, R. I.

[1]A. Kastler, Experimentia 8, 1 (1952).

[2]W. G. Proctor and W. H. Tantilla, Phys. Rev. 101, 1757 (1956).

[3]W. G. Robinson and W. A. Proctor, Phys. Rev. 104, 1344 (1956).

[4]D. A. Jennings, W. H. Tantilla, and O. Kraus, Phys. Rev. 109, 1059 (1958).

[5]E. F. Taylor and N. Bloembergen, Phys. Rev. 111, 431 (1959).

[6]D. I. Bolef and M. Menes, Phys. Rev. 114, 1441 (1959).

[7]M. Menes and D. I. Bolef, J. Phys. Chem. Solids 19, 79 (1961).

[8]A. H. Silver, J. Phys. Chem. Solids 23, 273 (1962).

[9]E. H. Gregory, NSF Tech. Rept. No. GP 2391 UCLA, 1965 (unpublished).

[10]E. H. Gregory and H. E. Bommel, Phys. Rev. Letters 15, 404 (1965).

[11]R. W. Mebs, L. H. Bennett, and J. R. Lidowitz, Phys. Letters 24A, 665 (1967).

[12]R. K. Sundfors, Phys. Rev. 177, 1221 (1969).

[13]K. Yosida and T. Moriya, J. Phys. Soc. Japan 11, 33 (1956).

[14]J. Kondo and J. Yamashita, J. Phys. Chem. Solids 10, 245 (1959).

[15]R. Sternheimer, Phys. Rev. 80, 102 (1950); 84, 244 (1951); and H. M. Foley, *ibid.* 92, 1460 (1953).

[16]J. C. Phillips, Rev. Mod. Phys. 42, 317 (1970).

[17]A. Abragam, *The Principles of Nuclear Magnetism* (Oxford U. P., London, 1961), p. 163.

[18]J. Van Kranendonk, Physica 20, 781 (1954).

[18a]We have estimated the contribution to $G(\theta)$ due to the neighbors (from second nearest to the sixth) to be 2% only.

[19]R. G. Barnes and W. V. Smith, Phys. Rev. 93, 95 (1954).

[20]R. Louden, Phys. Rev. 119, 919 (1960).

[21]R. K. Sundfors, Phys. Rev. 185, 458 (1969).

[22]F. N. H. Robinson, J. Sci. Instr. 36, 481 (1959).

[23]L. Wharton, L. P. Gold, and W. Klemperer, Phys. Rev. 133, B270 (1964).
[24]J. C. Browne and F. A. Matsen, Phys. Rev. 135, A1227 (1964).
[25]S. L. Kahalas and R. K. Nesbet, J. Chem. Phys. 39, 529 (1963).
[26]L. R. Suelzle, M. R. Yearian, and H. Crannell, Phys. Rev. 162, 992 (1967).
[27]T. P. Das and R. Behrsohn, Phys. Rev. 102, 733 (1956).
[28]A. Dalgarno, Advan. Phys. 11, 281 (1962).
[29]E. A. C. Lucken, *Nuclear Quadrupole Coupling Constants* (Academic, New York, 1969).
[30]J. Lahiri and A. Mukherji, Phys. Rev. 141, 428 (1965).
[31]F. W. Langhoff and R. P. Hurst, Phys. Rev. 139, A1415 (1965).
[32]J. Lahiri and A. Mukherji, Proc. Phys. Soc. (London) 87, 913 (1966).

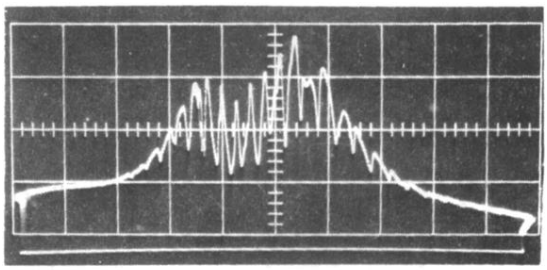

FIG. 2. Oscilloscope trace of the voltage developed across the *LC* tank circuit formed in part by the transducer sample assembly as the frequency sweeps from left to right across resonance. The deep dips correspond to mechanical resonance of the sample.